

The Measurement of Conductivity and Permittivity of Semiconductor Spheres by an Extension of the Cavity Perturbation Method*

K. S. CHAMPLIN†, MEMBER, IRE, AND R. R. KRONGARD†

Summary—A technique based on cavity perturbation theory is described with which one can determine the microwave conductivity and dielectric permittivity of a small sphere of completely arbitrary conductivity. These properties follow from the measured frequency shift and quality change occurring when the sample is inserted into a region of maximum electric field in a cavity resonator. The range of validity of the quasi-static internal field approximation is discussed, and curves are provided for extending the measuring technique beyond this range. The extended theory is valid for the entire conductivity range from zero to infinity. Measurements on several samples of known conductivity and permittivity in which the approximation is not satisfied are seen to agree with the theory. For highly conductive materials, the present method is closely related to the “eddy current loss” measuring technique discussed by others. The two methods are compared from the point of view of perturbation theory in order to determine their relative merits. Because the measuring technique employs a spherical sample, it may be applied profitably to materials with nonisotropic carrier mobilities and to semiconducting materials for which contact fabrication techniques are poorly known.

INTRODUCTION

C AVITY perturbation techniques have frequently been used to measure the complex magnetic and electric susceptibilities of many magnetic [1] and dielectric [2] materials. These measurements are performed by inserting a small appropriately shaped sample into a cavity resonator and determining the properties of the sample from the resultant change in quality and resonant frequency.

Such techniques have found very little use in research on materials with conductivities in the range of semiconductors. Several probable reasons are:

- 1) The assumption often made in perturbation calculations—that the fields are uniform throughout the sample—is usually not satisfied with semiconductors of practical size.
- 2) The conduction and displacement currents of semiconductors are often of the same order of magnitude at microwave frequencies. The simplifying assumptions which apply to either low-loss or high-loss materials are therefore not valid.
- 3) It is sometimes believed that the approximations inherent in perturbation methods preclude their use with materials of arbitrary conductivity.

* Received by the PGMTT, March 13, 1961; revised manuscript received, July 11, 1961. Supported by the AF Office of Scientific Research of the Office of Aerospace Research, under Contract No. AF 49(638)-747, and by the Graduate School of the University of Minnesota, Minneapolis.

† Dept. of Electrical Engineering, Institute of Technology, University of Minnesota, Minneapolis, Minn.

The present paper treats the problem of determining the microwave conductivity and permittivity of a small sphere (~ 1 mm radius for x -band measurements, as shown in Fig. 1) of completely arbitrary conductivity. These properties follow from the measured frequency shift and quality change occurring when the sample is inserted into a region of maximum electric field in a cavity resonator. The method is quite general and requires no *a priori* knowledge concerning the conductivity range of the sample. For materials of arbitrary conductivity, both the frequency shift and quality change are required to determine uniquely either the conductivity or the permittivity. Furthermore, the uniform internal field approximation often made in perturbation calculations is found to limit measurement to materials of low conductivity. A computer solution of the field equations removes this restriction, thus extending the measuring technique to high conductivity materials.

The measuring technique should apply to the systematic study of new semiconducting materials such as the organic semiconductors. For these materials, many of which have extremely nonisotropic carrier mobilities,

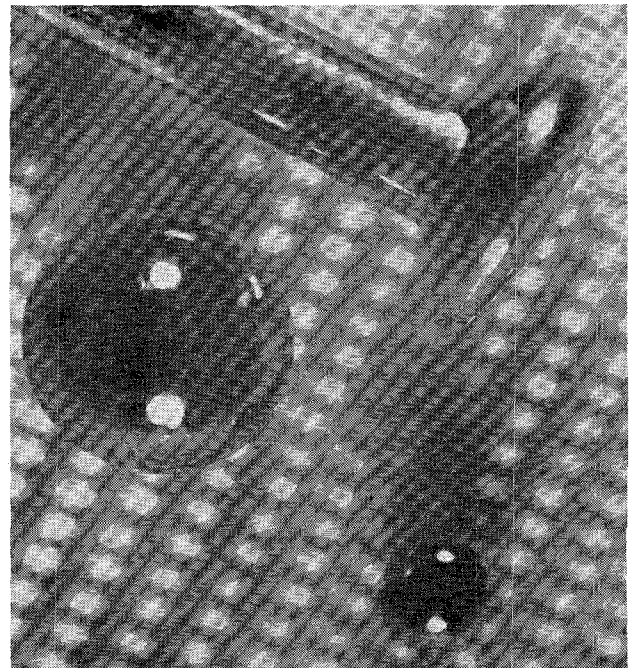


Fig. 1—Spherical samples of Si and Ge with radii of 1.0 mm and 0.4 mm, respectively. A common pin is included for size comparison.

the techniques of fabricating good "ohmic" contacts are totally unknown. In addition to the obvious advantage of eliminating contacts, the microwave technique has the further advantage of permitting measurement along various crystallographic directions by merely rotating the specimen.

I. THEORY

A. The Perturbation Formula

Consider a single oscillatory mode of a cavity resonator. If a perturbing specimen, small compared with the spatial variation of the unperturbed fields, is introduced into the cavity, the complex natural decay frequency changes by an amount [3]–[8]¹

$$\frac{\delta\hat{\omega}}{\hat{\omega}} = - \frac{\hat{\mathbf{P}} \cdot \hat{\mathbf{E}}_0^* + \hat{\mathbf{M}} \cdot \hat{\mathbf{H}}_0^*}{4W}, \quad (1)$$

where a complex quantity is denoted by a circumflex above it. In (1), $\hat{\mathbf{E}}_0$ and $\hat{\mathbf{H}}_0$ are the unperturbed fields at the location of the specimen, $\hat{\mathbf{P}}$ and $\hat{\mathbf{M}}$ are the specimen's total induced electric and magnetic moments observed externally, and W is the energy stored in the cavity. Although (1) applies to the transient case, measurements are generally obtained from the sinusoidal steady state. For the high- Q values of interest, these viewpoints are related by

$$\hat{\omega} = \omega_0 + j(\omega_0/2Q), \quad (2)$$

in which ω_0 is the resonant frequency for forced oscillations.

Placing the sample at an electric field maximum results in $\hat{\mathbf{H}}_0 = 0$, while the stored energy follows from the relation (mks units)

$$W = (1/2)\epsilon_0 \int_{\text{cavity}} |\hat{\mathbf{E}}|^2 dv \quad (3)$$

where $\hat{\mathbf{E}}$ is the unperturbed vector field distribution for the given mode. There remains only to determine $\hat{\mathbf{P}}$.

Casimir has solved for the magnetic moment of a ferromagnetic sphere in an initially uniform high-frequency magnetic field [9]. Because of the dual nature of Maxwell's equations, his solution applies also to the electric moment of a semiconducting sphere in a high-frequency electric field. The result, for a sphere of radius R and complex relative permittivity $\hat{\epsilon}_r$ is (see Appendix)

$$\hat{\mathbf{P}} = 3\epsilon_0 \left\{ \frac{\hat{\epsilon}_r \hat{\nu}(\hat{\gamma}R) - 1}{\hat{\epsilon}_r \hat{\nu}(\hat{\gamma}R) + 2} \right\} \left(\frac{4}{3} \pi R^3 \right) \hat{\mathbf{E}}_0, \quad (4)$$

¹ The integral form of the perturbation formula is derived in references [3]–[7]. For small samples, (1) and the more general integral form are equivalent.

in which $\hat{\gamma}$ is the propagation constant for plane waves in the material, and $\hat{\nu}(\hat{\gamma}R)$ is given by

$$\hat{\nu}(\hat{\gamma}R) = -2 \left\{ \frac{(\hat{\gamma}R) \cosh(\hat{\gamma}R) - \sinh(\hat{\gamma}R)}{(\hat{\gamma}R) \cosh(\hat{\gamma}R) - \{1 + (\hat{\gamma}R)^2\} \sinh(\hat{\gamma}R)} \right\}. \quad (5)$$

The imaginary part of the complex permittivity $\hat{\epsilon}_r$ results from both dielectric and conductive losses. For semiconductors in which conductive losses predominate,

$$\hat{\epsilon}_r = \epsilon_r - j\sigma_r \quad (6)$$

is a convenient convention, where the *relative conductivity* σ_r is equal to $\sigma/\omega\epsilon_0$ if dielectric losses can be neglected. The utility of this notation results from σ_r then being simply proportional to the conductivity in mks units, e.g., $\sigma_r = (0.53)\sigma$ at 9.6 kMc.

Because of the form of (4), we define the *effective* complex permittivity of the sphere by

$$\begin{aligned} \hat{\epsilon}_{r(\text{eff})} &= \hat{\epsilon}_r \hat{\nu}(\hat{\gamma}R) \\ &= \epsilon_{r(\text{eff})} - j\sigma_{r(\text{eff})}. \end{aligned} \quad (7)$$

Methods for converting from effective to actual values will be given in Section I-D. Combining (1), (3), (4) and (7) leads to

$$\frac{\delta\hat{\omega}}{\hat{\omega}} = - (3/2)(1/C_c)(v_s/v_c) \left[\frac{\hat{\epsilon}_{r(\text{eff})} - 1}{\hat{\epsilon}_{r(\text{eff})} + 2} \right], \quad (8)$$

where v_s and v_c are the volume of the sample and of the cavity, respectively, and C_c is the cavity constant,

$$C_c = \frac{1}{v_c} \int_{\text{cavity}} \left| \frac{\mathbf{E}}{\mathbf{E}_{\text{max}}} \right|^2 dv, \quad (9)$$

a quantity readily evaluated for a given mode; e.g., $C_c = \frac{1}{4}$ for a rectangular cavity oscillating in the TE_{10n} mode.

B. Inversion of the Perturbation Formula

Assuming that the Q of the perturbed resonator is fairly high, (8) may be written

$$\begin{aligned} \left\{ 1 + \frac{1}{K} \frac{\delta\omega_0}{\omega_0} \right\} + j \left\{ \frac{1}{K} \delta(1/2Q) \right\} \\ = \frac{3}{\{\epsilon_{r(\text{eff})} + 2\} - j\{\sigma_{r(\text{eff})}\}}, \end{aligned} \quad (10)$$

where

$$K = (3/2)(1/C_c)(v_s/v_c). \quad (11)$$

Eq. (10) is of the form of the complex transformation

$$\hat{Z} = 3/\hat{w}^*, \quad (12)$$

where $\hat{Z} = X + jY$ relates to the experimental parameters and $\hat{w} = u + jv$ to the physical properties of the

sphere. Separating (10) into real and imaginary parts yields

$$\left\{ 1 + \frac{1}{K} \frac{\delta\omega_0}{\omega_0} \right\} = \frac{3\{\epsilon_r(\text{eff}) + 2\}}{\{\epsilon_r(\text{eff}) + 2\}^2 + \{\sigma_r(\text{eff})\}^2}, \quad (13)$$

$$\left\{ \frac{1}{K} \delta(1/2Q) \right\} = \frac{3\{\sigma_r(\text{eff})\}}{\{\epsilon_r(\text{eff}) + 2\}^2 + \{\sigma_r(\text{eff})\}^2}. \quad (14)$$

The inverse transformation is, of course, of the same form. Thus

$$\{\epsilon_r(\text{eff}) + 2\} = \frac{3 \left\{ 1 + \frac{1}{K} \frac{\delta\omega_0}{\omega_0} \right\}}{\left\{ 1 + \frac{1}{K} \frac{\delta\omega_0}{\omega_0} \right\}^2 + \left\{ \frac{1}{K} \delta(1/2Q) \right\}^2}, \quad (15)$$

$$\{\sigma_r(\text{eff})\} = \frac{3 \left\{ \frac{1}{K} \delta(1/2Q) \right\}}{\left\{ 1 + \frac{1}{K} \frac{\delta\omega_0}{\omega_0} \right\}^2 + \left\{ \frac{1}{K} \delta(1/2Q) \right\}^2}. \quad (16)$$

Eqs. (15) and (16) separately yield $\epsilon_r(\text{eff})$ and $\sigma_r(\text{eff})$ from the measured changes in ω_0 and Q .

Fig. 2 shows the relative frequency shift and quality

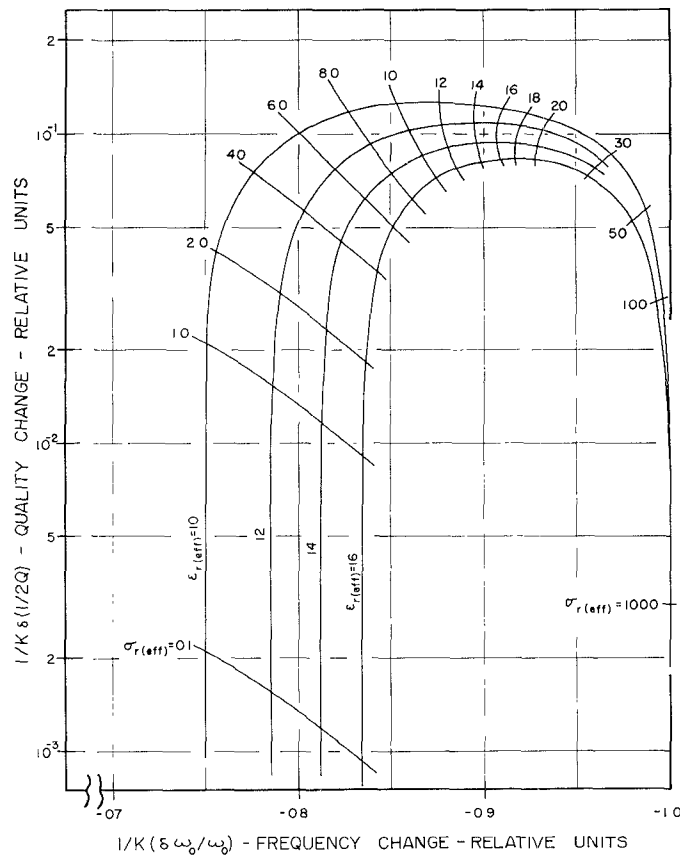


Fig. 2—Relative frequency shift and quality change as function of effective relative permittivity and conductivity of small semiconductor sphere. Sphere is placed at location of maximum electric field.

change for several values of $\epsilon_r(\text{eff})$ and $\sigma_r(\text{eff})$. For small $\sigma_r(\text{eff})$, the frequency change depends only on $\epsilon_r(\text{eff})$, and $\delta(1/Q)$ varies directly as $\sigma_r(\text{eff})$. Spencer, *et al.*, have measured the complex permittivity of small ferrite spheres with effective conductivities in this range [1]. At the other end of the $\sigma_r(\text{eff})$ scale, $\delta\omega_0/\omega_0$ approaches a constant independent of $\epsilon_r(\text{eff})$, while an inverse relationship exists between $\delta(1/Q)$ and $\sigma_r(\text{eff})$. One sees that in general, *both* experimental parameters are required to determine *either* $\epsilon_r(\text{eff})$ or $\sigma_r(\text{eff})$.

C. The Quasi-Static Field Approximation

Frequently, as in [1], one assumes that $|\hat{\gamma}R|$ is small compared with unity. The field distribution then follows from the static solution by merely extending ϵ_r to complex values. For a semiconducting sphere in an initially uniform time-varying field, the quasi-static field within the sphere is again uniform; and the sphere acquires an electric moment given by (4) with $\hat{v}(\hat{\gamma}R) = 1$. Thus, for the quasi-static case,

$$\begin{aligned} \epsilon_r(\text{eff}) &= \epsilon_r, \\ \sigma_r(\text{eff}) &= \sigma_r. \end{aligned} \quad (17)$$

The terms neglected in (4) by this approximation are those in $(\hat{\gamma}R)^2$ and higher orders.

The range of validity of the quasi-static approximation at 9.6 kMc can be determined from Fig. 3. If one limits $|\hat{\gamma}R|$ to values less than, say, $\frac{1}{2}$, a germanium sphere of $\frac{1}{2}$ -mm radius restricts measurement to resistivities greater than about 10 ohm-cm ($\sigma_r \lesssim 20$). Reducing the radius extends the range of validity. One can see, however, that practical considerations will prevent utilizing the quasi-static approximation with very low resistivity materials. For radii larger than about $\frac{3}{4}$ mm, the approximation is never valid regardless of the resistivity because of the large dielectric constant.

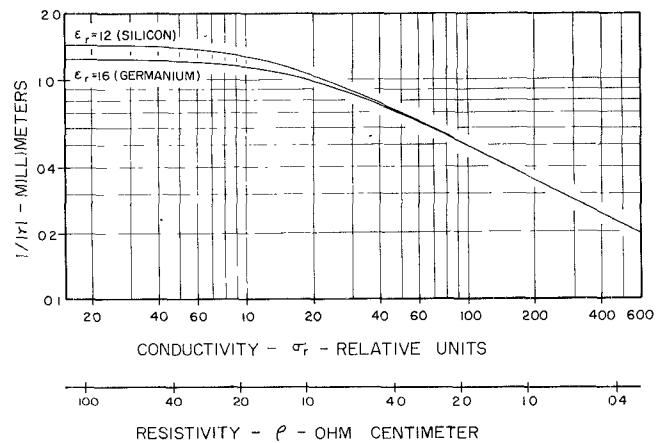


Fig. 3—Magnitude of inverse propagation constant as a function of conductivity for silicon and germanium. $f = 9.6$ kMc. For convenience, resistivity scale is also shown.

D. The Exact Solution—Conversion from Effective to Actual Values

For materials with magnetic permeabilities equal to unity, one can write

$$(\hat{\gamma}R) = j\omega(\mu_0\epsilon_0)^{1/2}(\hat{\epsilon}_r R^2)^{1/2}. \tag{18}$$

Since, at a given frequency, $(\hat{\gamma}R)$ is a function of the single complex variable $(\hat{\epsilon}_r R^2)$, (5) leads to the following complex relationship between $(\hat{\epsilon}_r R^2)$ and $(\hat{\epsilon}_{r(\text{eff})} R^2)$:

$$\{\hat{\epsilon}_{r(\text{eff})} R^2\} = -2\{\hat{\epsilon}_r R^2\} \cdot \left[\frac{(\hat{\gamma}R) \cosh(\hat{\gamma}R) - \sinh(\hat{\gamma}R)}{(\hat{\gamma}R) \cosh(\hat{\gamma}R) - \{1 + (\hat{\gamma}R)^2\} \sinh(\hat{\gamma}R)} \right]. \tag{19}$$

Eq. (19) has been evaluated for a frequency of 9.6 kMc with a high-speed digital computer. The results of these computations are shown in Figs. 4–6.

Figs. 4 and 5 show $a^2\epsilon_{r(\text{eff})}$ and $a^2\sigma_{r(\text{eff})}$ as functions of $a^2\epsilon_r$ and $a^2\sigma_r$, where a is the sphere radius in millimeters. At certain values, a type of dimensional resonance results in $\epsilon_{r(\text{eff})}$ changing sign. The positive range of $\epsilon_{r(\text{eff})}$ is shown in Fig. 4 and the negative range in Fig. 5. One sees from Fig. 5 that the results become less dependent on ϵ_r as σ_r increases. For $\epsilon_r \ll \sigma_r$, ($\rho \lesssim 1$ ohm cm for Ge and Si) a unique relationship exists between $a^2\sigma_{r(\text{eff})}$ and $a^2\sigma_r$, which is independent of ϵ_r . This relationship is shown in Fig. 6.

Although the curves of Figs. 4–6 were derived for $f=9.6$ kMc and $\mu_r=1$, one can easily extend their use to other frequencies and (real) permeabilities by introducing the “corrected” radius a' defined by

$$a' = \mu_r^{1/2} \frac{f(\text{kmc})}{9.6} a. \tag{20}$$

The plots in Figs. 4–6 are useful for estimating the accuracy of the quasi-static approximation as well as for converting from effective to actual values. As an example of the former, consider the solid curve $a^2\epsilon_r=4$ in Fig. 4 which applies to the $\frac{1}{2}$ -mm germanium sphere discussed in the previous section. At low conductivities, $\sigma_{r(\text{eff})}/\sigma_r=1.03$. As conductivity increases, the ratio decreases but is still about 0.925 for $a^2\sigma_r=80$ (Fig. 5). One concludes that with a $\frac{1}{2}$ -mm germanium sphere, the quasi-static approximation introduces less than 8 per cent error in the measured conductivity for $\sigma_r < 320$ ($\rho \gtrsim 0.6$ ohm-cm). Thus, as far as conductivity measurements are concerned, the quasi-static approximation is much less restrictive than one might assume from Fig. 3. For $\sigma_r > 320$, it becomes necessary to correct the effective conductivity. In this range, however, $\epsilon_r \ll \sigma_r$ so that Fig. 6 applies.

When the conductivity is large enough that $\epsilon_r \ll \sigma_r$ and $500 < a^2\sigma_r$ are simultaneously satisfied, the asymptotic approximation to the curve in Fig. 6 yields

$$a^2\sigma_{r(\text{eff})} = -a^2\epsilon_{r(\text{eff})} = \{5\sqrt{2}\} \{a^2\sigma_r\}^{1/2}, \tag{21}$$

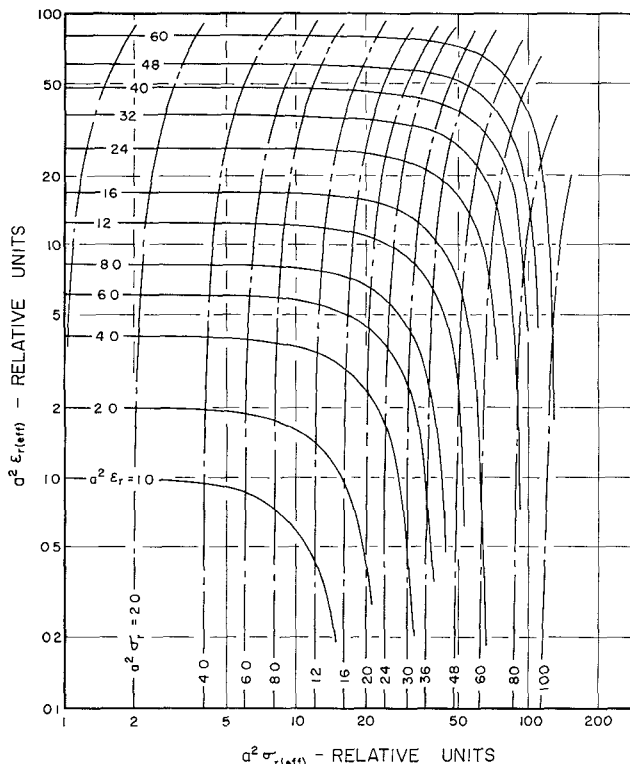


Fig. 4—Relationship between effective and actual values of relative permittivity and conductivity for sphere of radius a (millimeters) $f=9.6$ kMc, $\mu_r=1$, $\epsilon_r(\text{eff}) > 0$.

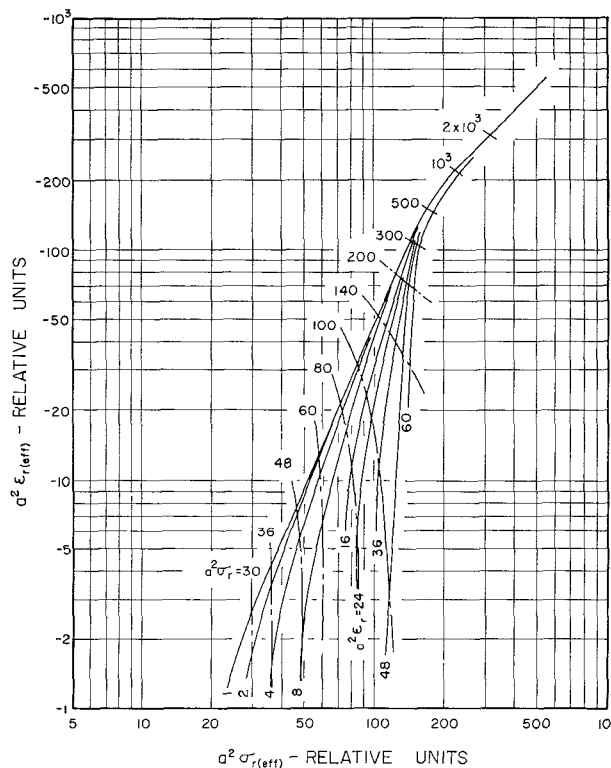


Fig. 5—Relationship between effective and actual values of relative permittivity and conductivity for sphere of radius a (millimeters). $f=9.6$ kMc, $\mu_r=1$, $\epsilon_r(\text{eff}) < 0$.

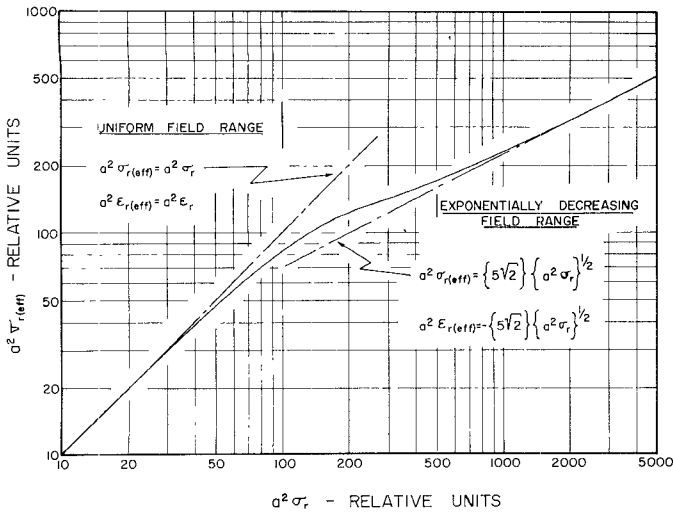


Fig. 6—Relationship between effective and actual relative conductivity for sphere of radius a (millimeters). $\epsilon_r \ll \sigma_r$, $f=9.6$ kMc, $\mu_r=1$.

while (13) and (14) become

$$\begin{aligned} \left\{ \frac{1}{K} \delta(1/2Q) \right\} &= - \left\{ 1 + \frac{1}{K} \frac{\delta\omega_0}{\omega_0} \right\} \\ &= \left(\frac{3}{2} \right) \frac{1}{\sigma_r(\text{eff})}. \end{aligned} \quad (22)$$

Combining, one has

$$\sigma_r = (0.045) \frac{a^2}{\left\{ \frac{1}{K} \delta(1/2Q) \right\}^2}. \quad (23)$$

Thus, for very high-conductivity materials, σ_r can be determined analytically from measurements of quality change alone.

E. The "Eddy Current Loss" Method

The conductivity of highly-conductive spheres can also be measured by the "eddy current loss" method. With this method, one determines the conductivity from the change in Q which results from inserting the sample into a region of maximum magnetic field in a cavity resonator.

The eddy current loss method was first discussed by Linhart, *et al.*, who analytically determined the conductivity of a sphere that was large compared with the skin depth [10]. The size restriction was later removed by Kohane and Servitz with a graphical evaluation procedure [11]. Both papers contain the tacit assumption which led to Fig. 6; *i.e.*, $\epsilon_r \ll \sigma_r$ ($\rho \gtrsim 1$ ohm-cm for Si and Ge). Further, the method of Linhart, *et al.*, applies to the region $500 < a^2\sigma_r$, for which the asymptotic approximation in Fig. 6 and (23) are justified.

For comparison with the "standard" method, it is informative to discuss the eddy current loss method from the standpoint of perturbation theory. According

to Casimir [9], a sphere of relative permeability $\hat{\mu}_r$ in a high-frequency magnetic field acquires a magnetic moment

$$\hat{M} = 3\mu_0 \left[\frac{\hat{\mu}_r \hat{\nu}(\hat{\gamma}R) - 1}{\hat{\mu}_r \hat{\nu}(\hat{\gamma}R) + 2} \right] \left\{ \frac{1}{3} \pi R^3 \right\} \hat{H}_0, \quad (24)$$

in complete analogy with (4). Again, $\hat{\nu}(\hat{\gamma}R)$ is defined by (5). Since electric and magnetic fields enter (1) in exactly the same way, the work in Sections I-A and I-B can be extended to the present case by merely redefining the cavity constant in terms of magnetic fields and replacing $\hat{\epsilon}_r(\text{eff})$ with $\{\hat{\mu}_r \hat{\nu}(\hat{\gamma}R)\}$. For nonmagnetic materials ($\hat{\mu}_r \cong 1$), as considered in references [10] and [11], one then has the following:

- 1) The real part of $\hat{\nu}(\hat{\gamma}R)$ replaces $\epsilon_r(\text{eff})$,
- 2) The imaginary part of $\hat{\nu}(\hat{\gamma}R)$ replaces $-\sigma_r(\text{eff})$.

Performing these substitutions in (14) and evaluating for $\epsilon_r \ll \sigma_r$ leads to the transcendental equation which has been plotted by Kohane and Servitz [11].

For large $|\hat{\gamma}R|$, $\hat{\nu}(\hat{\gamma}R)$ approaches $2/(\hat{\gamma}R)$. The transcendental expression then becomes

$$\begin{aligned} \left\{ \frac{1}{K} \delta(1/2Q) \right\}_e &= \frac{3}{2\sqrt{2}} \frac{1}{\omega(\mu_0\epsilon_0)^{1/2}R} \frac{1}{\sigma_r^{1/2}}, \end{aligned} \quad (25)$$

in agreement with Linhart, *et al.* [10]. For the same approximation, the standard method leads to [see (23)]

$$\left\{ \frac{1}{K} \delta(1/2Q) \right\}_s = \frac{3}{2\sqrt{2}} \omega(\mu_0\epsilon_0)^{1/2}R \frac{1}{\sigma_r^{1/2}}. \quad (26)$$

Thus, at 9.6 kMc the observed quality change by the two methods has the ratio

$$\frac{\left\{ \frac{1}{K} \delta(1/2Q) \right\}_e}{\left\{ \frac{1}{K} \delta(1/2Q) \right\}_s} = \left(\frac{5}{a} \right)^2, \quad (27)$$

where a is the sphere radius in millimeters.

The following comparisons can now be made:

1) The standard method has several advantages over the eddy current loss method if the conductivity is not too large. The standard method is useful over a very wide conductivity range; it may be used with materials with $\mu_r \neq 1$; and unlike the eddy current loss method, it gives a single valued result.

2) On the other hand, the eddy current loss method is probably preferable for conductivity measurements in the range $500 < a^2\sigma_r$, because there is a larger quality change for a given σ_r than with the standard method if the radius is less than 5 mm (as the original assumptions require). The eddy current loss method should thus yield greater accuracy in this conductivity range.

TABLE I
TYPICAL MEASUREMENTS

	ρ_{dc} Ω cm	a mm	δP db	δf mcs	$a^2\epsilon_r(\text{eff})$	$a^2\sigma_r(\text{eff})$	$a^2\epsilon_r$	$a^2\sigma_r$	ϵ_r	ρ Ω cm
Sample 1 n-type Si	250	0.945	1.94	10.39	11.12	0.743	10.4	0.683	11.6	248
Sample 2 p-type Si	135	1.026	4.03	13.30	12.91	1.58	12.3	1.47	11.6	136
Sample 3 n-type Ge	37	1.55	9.13	20.49	22.12	8.32	21.12	6.90	15.9	36.3
Sample 4 n-type Ge	10	0.982	9.81	13.96	13.47	21.78	15.0 ± 1	19.8	15.6 ± 1	9.8
Sample 5 n-type Si	3	1.033	7.27	17.39	-1.43	67.22	15 ± 5	65.0	15 ± 5	3.1

II. EXPERIMENTAL RESULTS

Measurements of microwave conductivity and permittivity have been performed on a number of single-crystal germanium and silicon specimens. An under-coupled, rectangular transmission cavity, oscillating in the TE_{103} mode, was used in these studies. The sample was placed on a slight indentation in the center of a thin mylar film stretching horizontally across the middle of the cavity. The film supported the sample at the cavity's geometric center, yet left the empty cavity field relatively undisturbed. Opening and closing the cavity during measurement was avoided by inserting the sample through a small hole at a region of minimum wall current. The empty cavity had a resonant frequency of 9.482 kMc, a loaded Q of 7650, and a volume of 15.18 cm³.

The response curve of the cavity was displayed on an oscilloscope by frequency modulating the klystron source. A marker pulse indicating the absorption frequency of a cavity wavemeter was superimposed on this resonance curve and used for measuring frequency differences. The change in quality caused by the sample was determined from the change in transmitted power as measured with a precision attenuator by using the following relation [12]:

$$\delta(1/2Q) = \frac{1}{2Q_0} \left[\left(\frac{P_1}{P_0} \right)^{1/2} - 1 \right], \quad (28)$$

where Q_0 is the loaded Q of the empty cavity.

Typical results are shown in Table I. Even for the samples with large resistivity, the quasi-static approximation is not justified in these measurements since $|\hat{\gamma}R|$ is of the order of unity (see Fig. 3). The approximation gets worse as resistivity decreases. Indeed, for sample 5, the effective permittivity is actually negative. Although permittivity measurements are rather inaccurate in this range, the corrected value is of the right order of magnitude. The agreement between values of resistivity measured by dc and by microwave means is seen to be excellent.

III. CONCLUSIONS

The preceding discussion has developed the relationships between the electrical properties of a small sphere of completely arbitrary conductivity and the frequency shift and quality change resulting from its insertion into a cavity resonator. For experiments in which the quasi-static field approximation is justified, the inversion formulas (15) and (16) yield the conductivity and permittivity of the sphere in terms of the experimental parameters. For the general case, however, (15) and (16) yield only "effective" values which are then converted to the "actual" conductivity and permittivity with the aid of Figs. 4-6. Measurements on materials not satisfying the quasi-static approximation show good agreement with the theory.

The above method may possibly be applicable to the observation of such semiconductor phenomena as the photoconductive effect, the magnetoresistive effect, and the "hot" electron effect, as well as to the simpler measurement of static conductivity. Since "ohmic" contacts are not used, these measurements can be made on materials for which contact fabrication techniques are not well understood. Furthermore, the spherical geometry should allow one to perform separate electrical measurements along the various crystal axes of non-isotropic solids by merely rotating a single specimen.

APPENDIX

THE ELECTRIC MOMENT OF A SEMICONDUCTING SPHERE IN A TIME-VARYING ELECTRIC FIELD

Consider a sphere of radius R in a time-varying electric field. Assume that the sphere is sufficiently small so that the external field in its neighborhood is quasi-static, reducing to a uniform field in the Z direction \hat{E}_{z0} at large distances. Since the magnitudes of the constitutive parameters are to be unrestricted, no such assumption will apply to the internal field. This problem, whose magnetic analogue has been discussed by Casimir [9], is thus a step beyond the quasi-static treatment.

In view of the solenoidal character of the complex dis-

placement vector, it can be derived from a vector potential \hat{A} whose divergence is zero. Thus

$$\left. \begin{aligned} \epsilon(\mathbf{r})\hat{E} &= \nabla \times \hat{A} \\ \nabla \cdot \hat{A} &= 0 \end{aligned} \right\} \quad (29)$$

and

$$\epsilon(\mathbf{r}) = \begin{cases} \epsilon_0 & \text{for } R < r \\ \epsilon_0\epsilon_r & \text{for } r < R. \end{cases} \quad (30)$$

The vector potential satisfies

$$\nabla^2 \hat{A} = 0 \quad \text{for } R < r \quad (31)$$

$$\nabla^2 \hat{A} - \gamma^2 \hat{A} = 0 \quad \text{for } r < R \quad (32)$$

with

$$\gamma = j\omega\{\mu_0\epsilon_0\epsilon_r\}^{1/2},$$

and the boundary conditions that \hat{A} and the tangential component of \hat{E} are continuous at the surface of the sphere.

Just as in the quasi-static treatment, the external field is the superposition of the uniform field \hat{E}_{z0} and that of a dipole in the z direction with moment \hat{P}_z .

$$\left. \begin{aligned} A_x &= - (1/2)\epsilon_0\hat{E}_{z0}y - \hat{P}_z \frac{y}{4\pi r^3} \\ A_y &= + (1/2)\epsilon_0\hat{E}_{z0}x + \hat{P}_z \frac{x}{4\pi r^3} \end{aligned} \right\} \quad (33)$$

Inside the sphere, we put formally

$$\left. \begin{aligned} A_x &= - \hat{j}(\gamma r)y, \\ A_y &= + \hat{j}(\gamma r)x. \end{aligned} \right\} \quad (34)$$

Substituting (34) into (32) leads to

$$\hat{j}'' + \frac{4}{(\gamma r)}\hat{j}' - \hat{j} = 0 \quad (35)$$

which has the solution

$$\begin{aligned} \hat{j}(\gamma r) &= a \left\{ \frac{(\gamma r) \cosh(\gamma r) - \sinh(\gamma r)}{(\gamma r)^3} \right\}, \\ &= a\hat{\mu}(\gamma r) \end{aligned} \quad (36)$$

where a is a constant to be determined from boundary conditions.

From the continuity of \hat{A} at the surface one has

$$a\hat{\mu}(\gamma R) - \frac{\hat{P}_z}{4\pi R^3} = (1/2)\epsilon_0\hat{E}_{z0}, \quad (37)$$

and from the continuity of the tangential component of \hat{E} ,

$$\frac{a}{\epsilon_r} \{ 2\hat{\mu}(\gamma R) + (\gamma R)\hat{\mu}'(\gamma R) \} + \frac{\hat{P}_z}{4\pi R^3} = \epsilon_0\hat{E}_{z0}. \quad (38)$$

Solving (37) and (38) for \hat{P}_z yields the desired result,

$$\hat{P}_z = 3\epsilon_0 \left\{ \frac{\epsilon_r\hat{\nu}(\gamma R) - 1}{\epsilon_r\hat{\nu}(\gamma R) + 2} \right\} \left(\frac{4}{3} \pi R^3 \right) \hat{E}_{z0}, \quad (39)$$

where

$$\hat{\nu}(\gamma R) = \frac{2\hat{\mu}(\gamma R)}{2\hat{\mu}(\gamma R) + (\gamma R)\hat{\mu}'(\gamma R)} \quad (40)$$

$$\hat{\nu}(\gamma R) = -2 \left\{ \frac{(\gamma R) \cosh(\gamma R) - \sinh(\gamma R)}{(\gamma R) \cosh(\gamma R) - \{1 + (\gamma R)^2\} \sinh(\gamma R)} \right\}. \quad (41)$$

ACKNOWLEDGMENT

The authors would like to thank J. E. Holte for his helpful assistance in programming the Univac 1103 digital computer and to D. Long of the Minneapolis Honeywell Research Center, Minneapolis, Minn., for supplying the bulk semiconductor samples upon which the measurements were made.

REFERENCES

- [1] See, e.g., E. G. Spencer, R. C. LeCraw, and F. Reggia, "Measurement of microwave dielectric constants and tensor permeabilities of ferrite spheres," *Proc. IRE*, vol. 44, pp. 790-800; June, 1956.
- [2] G. Birnbaum and J. Franeau, "Measurement of the dielectric constant and loss of solids and liquids by a cavity perturbation method," *J. Appl. Phys.*, vol. 20, pp. 817-818; August, 1949.
- [3] J. Müller, "Untersuchung über Elektromagnetische Hohlräume," *Z. Hochfrequenztech. Elektroak.*, vol. 54, pp. 157-161; 1939.
- [4] H. A. Bethe and J. Schwinger, Cornell University, Ithaca, N. Y., NDRC Rept. D1-117; 1943.
- [5] J. C. Slater, "Microwave electronics," *Rev. Mod. Phys.*, vol. 18, pp. 441-512; October, 1946.
- [6] H. B. G. Casimir, "On the theory of electromagnetic waves in resonant cavities," *Philips Research Repts.*, vol. 6, pp. 162-182; June, 1951.
- [7] R. A. Waldron, "Perturbation theory of resonant cavities," *Proc. IEE*, vol. 107C, pp. 272-274; September, 1960.
- [8] C. H. Papas, "Thermodynamic consideration of electromagnetic cavity resonators," *J. Appl. Phys.*, vol. 25, pp. 1552-1553; December, 1954.
- [9] H. B. G. Casimir, "On the theory of eddy currents in ferromagnetic materials," *Philips Research Repts.*, vol. 2, pp. 42-54; February, 1947.
- See also N. Bloembergen, "On the magnetic resonance absorption in conductors," *J. Appl. Phys.*, vol. 23, pp. 1383-1389; December, 1952.
- See also J. O. Artman, "Effects of size on the microwave properties of ferrite rods, discs and spheres," *J. Appl. Phys.*, vol. 20, pp. 92-98; January, 1957.
- [10] J. G. Linhart, I. M. Templeton and R. Dunsmuir, "A microwave resonant cavity method for measuring the resistivity of semiconducting materials," *Brit. J. Appl. Phys.*, vol. 7, pp. 36-37; January, 1956.
- [11] T. Kohane and M. H. Sirvetz, "The measurement of microwave resistivity by eddy current loss in small spheres," *Rev. Sci. Instr.*, vol. 30, pp. 1059-1060; September, 1959.
- See also T. Kohane, "The measurement of microwave resistivity by eddy current loss in small spheres," *IRE TRANS. ON INSTRUMENTATION*, vol. I-9, pp. 184-186; September, 1960.
- [12] C. J. Montgomery, R. H. Dicke and E. M. Purcell, Eds., "Principles of Microwave Circuits," M.I.T. Rad. Lab. Ser., McGraw-Hill Book Co., Inc., New York, N. Y., 288 pp.; 1948.